Blade Analysis of HAWT Using BEMT Approach

Prof. Kumbharkar Vijaykumar[1], Prof. Chaudhari Bharat[2]
[1, 2] Department of Mechanical Engineering
[1, 2] Sinhgad Institute of Technology, Lonavala

Abstract- *Wind energy is an abundant natural resource that people have been trying to tap in recent decades. More and more wind turbines are being built to solve the world's energy shortage problem. This paper shows the results of a computational fluid dynamic simulation developed to predict the air flow field and associated aerodynamic quantities around the moving blades of a wind turbine. There have been various researches using CFD to identify the blade performance and flow characteristics. As CFD analysis utilizes the three-dimensional Navier-Stokes equation as the governing equation, it has the advantage of providing more accurate result of analysis compared to previous aero-elastic code. On the contrary, to acquire reliable result from computational method, a vast amount of computational grids are required and advanced turbulence model needs to be applied. The computational method is very useful for understanding the aerodynamic characteristics of rotor blades, but it consumes too much time and resources; thus it is generally applied at the final performance evaluation stage after all the design process is completed. In this study, aerodynamic design for variable -speed variable pitch type 3 -MW wind turbine blade was completed and analysis results by BEMT and CFD were compared. In addition, flow characteristics on the blade surface will be presented for reference.*

Keywords- wind turbine, aerodynamic, wind speed, rotor

I. INTRODUCTION

A wind turbine uses rotor blades to extract and convert kinetic energy of wind into electrical energy. Therefore, a rotor blade requires optimal aerodynamic shape to maximize its efficiency and to improve power performance. There have been various researches using computational fluid dynamics (CFD) to identify the blade performance and flow characteristics. As CFD analysis utilizes the three-dimensional Navier-Stokes equation as the governing equation, it has the advantage of providing more accurate result of analysis compared to previous aero-elastic code. On the contrary, to acquire reliable result from computational method, a vast amount of computational grids are required and advanced turbulence model needs to be applied. The computational method is very useful for understanding the aerodynamic characteristics of rotor blades, but it consumes too much time and resources; thus it is generally applied at the final performance evaluation stage after all the design process is completed. In this study, aerodynamic design for variable -speed variable pitch type 3 -MW wind turbine blade was completed and analysis results by BEMT and CFD were compared. In addition, flow characteristics on the blade surface are presented for reference.

II. HORIZONTAL AXIS WIND TURBINE

The Horizontal Axis Wind Turbines (HAWT) when compared to the Vertical Axis Wind Turbines (VAWT), the HAWTs

1. Present higher values of power coefficients.
2. Operate in the high Atmospheric Boundary Layer instead of the bottom shear layer, so they see more uniform and intense wind speeds.
3. Have a more stable mechanical behavior and they can assume larger sizes.

Although they were widely investigated in the 1980's, VAWTs have not proved to be commercially competitive and are not currentlymanufactured in significant number. Additional information about VAWTs characteristics can be found in.

2.1 Wind power technology

Nowadays, wind turbines are the largest rotating machines on earth. The world's largest passenger's airliner, i.e. the Airbus A-380, has a wing span of about 80m, whereas an Enercon E-126/6 MW wind turbine (the world's most powerful WT) has a rotor diameter of 126 m which, being the tower even 138 m tall makes this machine reach 200 m of overall height from tower base to blade tip. They are also the oldest devices for exploring the energy of the wind on land. In fact, the only older device for utilizing wind energy in general is the sailing ship.

Mankind has needed for centuries mechanical energy, mainly for agriculture, and increasingly. In order to extract a useful form of energy from wind, that he saw free flowing everywhere, proper machines were necessary and here is how windmills born. Today after decades of running industrial development, modern turbines transform the same energy to electric power that has already become no replaceable for human life in the 21st century. Moreover, the huge and still

increasing size causes their design to be a real challenge for engineers.

The knowledge about the wind power technology has increased over the years; the development of various windmill types from middle- Ages to the industrial era can hardly be considered the result of a systematic research and development. However, as late as the 17th and 18th century, when physical—mathematical thinking became more established, systematic considerations on windmill technology took their beginnings. Among the other, Leonardo, Leibniz, Bernoulli and Euler involved themselves in the matter. In about 1890 the Danish professor Poul La Cour carried out extensive scientific research in windmill blade aerodynamics and windmill design, turning later his experiments to how to generate electrical current with the help of wind power. Like no other he marked the turning point from historical windmill building to the modern technology of power generating wind turbines. Lanchester (1915) and Betz (1920) were the firsts to predict the maximum power output of an ideal wind turbine, by applying the principle that for the extraction of mechanical energy from an air flow the exact geometry of the energy converter is physically irrelevant. A similar approach had already been developed by Froude and Rankine at the end of the 19th century, but for ship propellers.

2.2 Wind turbine parts

The main parts of a wind turbine parts as shown in fig. 1 are:

1. **BLADES:** or airfoil designed to capture the energy from the strong and fast wind. The blades are lightweight, durable and corrosion -resistant material. The best Materials are composites of fiberglass and reinforced plastic.
2. **ROTOR:** designed to capture the maximum surface area of wind. The rotor rotates the generator through the low speed shaft and gear box.
3. **GEAR BOX:** A gear box magnifies or amplifies the energy output of the rotor. The gear box is situated directly between the rotor and the generator.
4. **GENERATOR:** The generator is used to produce electricity from the rotation of the rotor. Generators come in various sizes, relative to the desired power output.
5. **NACELLE:** The nacelle is an enclosure that seals and protects the generator and gear box from the other elements.
6. **TOWER:** The tower of the wind turbine carries the nacelle and the rotor. The towers for large wind turbines may be either tubular steel towers, lattice towers, or concrete towers. The higher the wind tower, the better the wind. Winds closer to the ground are not only slower, they are also more turbulent. Higher winds are not corrupted by obstructions on the ground and they are also steadier.

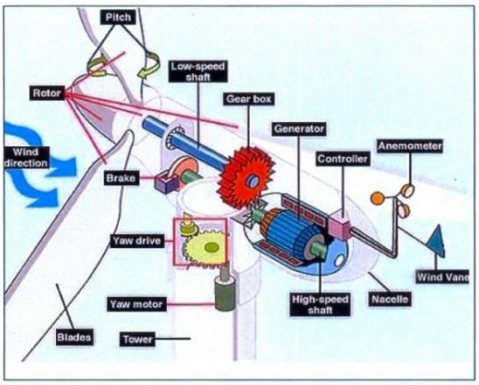

Fig. 1 - Configuration of a typical HAWT

2.3 Working of HAWT

In this section the basics of the functioning of modern HAWT are briefly summarized. Since the transformation of wind energy into electricity is not obtained directly, but consists of many complicated steps (and passing through the mechanical energy form). The latest technologies of aerodynamics, mechanics, control systems and electro technology are involved in such process. The figure 2 shows power generation process of a wind turbine. Wind turbine blades are affected by a force distribution, which results in a mechanical torque at the rotor shaft and the rotor itself rotates. In modern airscrew that aerodynamic driving force is mainly a lift force, like for the air-craft flight, rather than drag force like it is in ancient sailing ships. The shaft transfers the torque from the blades to the generator, but this passage can be achieved indifferent ways.

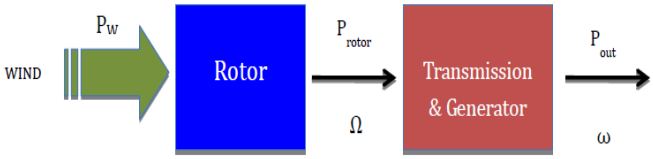

Fig.2 - Power generating process of a o wind turbine [14]

III. CFD AND WIND TURBINES

3.1 Introducing CFD

With Computational Fluid Dynamics we indicate the numerical solution of the differential governing equations of fluid flows, with the help of computers. This technique has a wide range of engineering applications. In the field of aerodynamic research this technique has become increasingly important and it is prominent for studying turbo machinery.

A number of valuable advantages are achieved following a CFD approach to a fluid dynamic problem:

1. CFD is faster and definitely cheaper. A considerable reduction of time and costs for solving the problems is offered compared to the traditional approaches. A conscious assessment of different solutions is available in the early phase of the design process, in order to fit with the requested tasks. Thus, experimental tests would be done just on few models, resulted from the CFD analysis.
2. Full-size analysis is hard to perform for large systems, like modern wind turbines are, or for extreme thermo-flow conditions as well as narrow geometries. A CFD study is a favorable choice in these cases.
3. A key—important quality of CFD are the detailed solutions allowed by the recent techniques (and computer technologies), even for time -dependent flows and complex systems.
4. The numerical models of the physical problems have good accuracy and reliability, due again to the newest mathematical improvements of solution schemes and of turbulence models.
5. Due to the last two advances, in most of the cases the prediction of a fluid dynamic problem does not require a dedicated powerful workstation and sometimes a personal computer might be sufficient.

The numerical modeling of a fluid dynamics problem implicates first a precise reading of the physical phenomena. All the relevant features of interest should be indicated at that first step, including geometry, materials, boundary conditions, to be defined in the simplest way, but without introducing extreme errors with the hypothesis. Nevertheless, a number of simplifications is always accepted, and is inevitable in order to model properly fluid dynamics problems.

3.2 The structure of a CUD code

A comprehensive overviews of the techniques used to solve problems in fluid mechanics on computers. In commercial codes a friendly interface gives the user the possibility of easy setting the various options and analyzes the results. Three large parts are generally indicated of a CFD code, which correspond to three phases of the problem analysis:

3.2.1 Preprocessor

In this phase the physical problem is implemented into the mathematical model. The computational domain is now defined. Then, it is divided into a certain number of elements, which constitute the mesh or grid. The fluid properties and the boundary conditions are set. Since the CFD solution of a fluid dynamic problem is given locally, for well—defined positions within computational grid, the global accuracy strongly depends on the total number of mesh elements. A rule-of-thumb says the larger is the number of elements; the better is the solution accuracy, even though CPU effort and the total time of convergence will be higher as well. Consequently, the optimal grid should not be uniform, but finer where higher are the variables gradients and coarser in the region characterized by smooth changes in the flow. The final success of a CFD simulation strongly depends on the preprocessing and therefore a special attention might be paid to the choice of the mesh and of boundary conditions.

3.2.2 Solver

The numerical solution algorithm is the core of a CFD code. All the main CFD solvers work with the following procedure:

1. Modeling the problem unknowns by means of simple analytical functions.
2. Discretizing the governing equations for the fluid flows, properly modified by substituting the former mentioned functions.
3. Solving the algebraic system of equations. Most of the commercial CFD codes (e.g. FLUENT) are based on a finite volume discretization and perform these operations:
4. Integrating the governing equations over each control volume within the computational domain. In the resulting equations, the flux terms figure.
5. Discretizing: the flux tenns, which deal with convection and diffusion processes, are approximated with a finite differential approach as well as the source terms when being present, in order to obtain an algebraic system of equations.
6. Solving the algebraic system of equations with iterative methods.

3.2.3 Post –processing

Under this definition we include the analysis of solution results. The solver output is a set of solution variables, associated to the given grid nodes or volumes. These data must be collected, elaborated in the most suitable way for the analysis, in order to produce a physical representation of the solution. Some CFD software package (like Fluent for instance) contains a post -processing section. Other solvers need an external tool for data treatment, which can be a commercial one (several complete packages exist for the scope) or a dedicated in—house code.Anyhow, one might be able to do the following post-processing operations:

1. Domain and grid visualization
2. Vectorial plots of solution variables
3. Linear, surface, volume integrals
4. Iso-level and contour plots of solution variables, within selected domain zones
5. Drawing two-dimensional and three-dimensional plots
6. Tracking path -lines, stream traces, etc.
7. Algebraic and analytical operations within the variables
8. Dynamic representations, animations etc.

In general, we should refer to the solved flow field as it had been an experimental test situation. Among the given data set, we could operate as we were using real instruments, by selecting the position of "virtual" probes or control surfaces where our interest is focused.

3.3 RANS equations

When approaching the study of fluid dynamics problems, the mathematical model is based on the fundamental mass, momentum and energy conservation principles. Therefore, the conservation laws are invoked in the following, in the vectorial notation and conservative form for unsteady, three—dimensional compressible flow.

The equations for conservation of mass, or continuity equation, can be written as follows

$$\frac{\partial \rho}{\partial t} + \nabla . (\rho \vec{v}) = Sm \qquad (1)$$

Where Sm is a mass source and the conservation of momentum is

$$\frac{\partial}{\partial t}(c\vec{v}) + (\rho \vec{v}\vec{v}) = -\nabla p + \nabla.(\bar{\bar{\tau}}) + \rho \vec{g} + \vec{F} \qquad (2)$$

Where ρ the static pressure, is the stress tensor (described below), ρg is the gravity force and F is the other external body forces. By assuming the Stokes' hypothesis for Newtonian fluids, the stress tensor τ is given by

$$\bar{\bar{\tau}} = \mu \left((\nabla \vec{v} + \nabla \vec{v} T) - \frac{2}{3} \nabla . \ \vec{v} I \right) \quad (3)$$

These above are named as Navier-Stokes equations. According to Reynolds, for each of the instantaneous dependent variables in the NS equations a time—average and a randomly fluctuating component can be found, for instance the velocity i-component will be

$$u_i = \bar{u}_l + u_i' (4)$$

Where u_i is time averaged component and u_i' is the fluctuating one. The time-averaged term is obtained by means of the Reynolds' time -average operator, which locally applied to the velocity vector reads

$$\bar{u}_l = \frac{1}{\Delta t} \int_{t_0}^{t_0 + \Delta t} u_i dt (5)$$

After applying the previous expression to the whole variable set in the NS equations, the incompressible time -averaged NS or incompressible RANS equations results. For compressible flows an analogous set of equation results by applying in addition a mass-averaging operator [11].

3.4 Wind turbine parameters

Parameters to design wind turbine is discussed in this session. Parameters like rated power, rated wind speed, diameter number of blades, design class, generator speed, rotor speed,material, power loss tip speed ratio and gear ratio is to be considered.

3.4.1 Initial design conditions

Table 1 - Basic design parameter [17]

Rated power	3MW	Swept area	7058 m^2
Rated wind speed	12.1 m/s	Rotor speed	15.11 rpm
Diameter	94.8 m	Material	GERP
Number of blades	3	Power loss	0.855
Design class	IB	λ_{design}	7.5
Generator Speed	1800 rpm	Gear ratio	1:131

Wind turbine class is defined as the values of reference wind speed (V_{ref}) and turbulence intensity (I15). Reference wind speed is the 10 minutes -averaged value for extreme wind speed which has the recurrence period of 50 years at the height of hub, and turbulence intensity is the value of turbulence intensity with the condition of 10minutes averaged wind speed of 15 m/s at the height of hub.

By considering the blade design for offshore wind power generation IEC Class IB has selected (high reference wind speed and low turbulence intensity).

Table 2 - Final development goal of 3MW blade [17]

Items	Specifications
Diameter / mass	94.8 m (11 – 12 ton)
External environmental condition	IEC class IB, 2nd edition
Power output	3MW (V_{rated} = 12 m/s)
Efficiency	About 0.5 (aerodynamic)

Table 1 shows the initial design factors for 3 MW blades calculated from nominal generator speed of 1800 rpm and gear ratio of 1:131. λ_{design} is defined as design tip speed ratio which is normally set at the range of 7 ~ 9 in large wind turbines; as the value ofλ_{design} gets bigger, the blade will be more slender and flexible. A slender blade has the advantage of reducing the load; however, it may cause an interference problem between tower and blade at extreme wind condition and the blade rotation speed may need to be increased to acquire the targeted power output. On the contrary, with a smaller value of λ_{design} , the blade will be thickened and it causes greater axial thrust force. Therefore, it is very important to set the proper value of λ_{design} [4]

3.4.2 Computational grid and domain

Neither the tower nor the ground was included into the model, and a uniform wind speed profile was assumed at the entrance of the domain. To generate the volume mesh for the three bladed rotors, the 120 degrees periodicity of the rotor was exploited, by only meshing the volume around one blade. The remaining two blades were included in the computations using periodic boundary conditions. The pre-processor GAMBIT 6.0 was used to build a tetrahedral mesh of approximately 1.25million volumes.

The computational domain was conical shaped, extending in the axial direction roughly 10 diameters upstream and 20 diameters downstream of the rotor. In the plane of the rotor, the domain diameter was ten times that of the rotor. These dimensions have been resulted from a dedicated study on outer boundaries dependency as shown in figure 3. While keeping the first narrow dimensions, the rotor worked as inducted configuration, resulting in a sensible over -prediction of the overall performance(nearly +10% respects to the largest domain, in design conditions). Moreover, the flow tended to accelerate in between the rotor disc and the boundaries, so that the wake too resulted affected by the vicinity of the boundary.

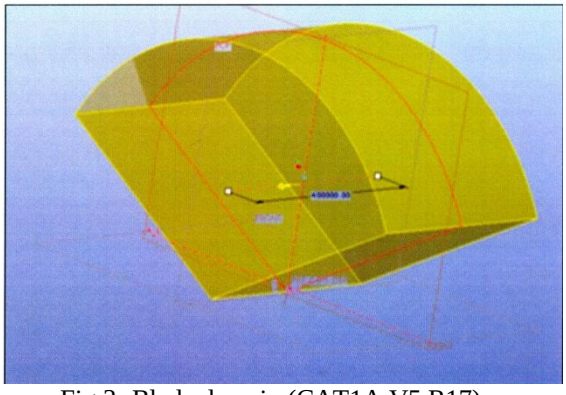

Fig.3- Blade domain (CAT1A V5 R17)

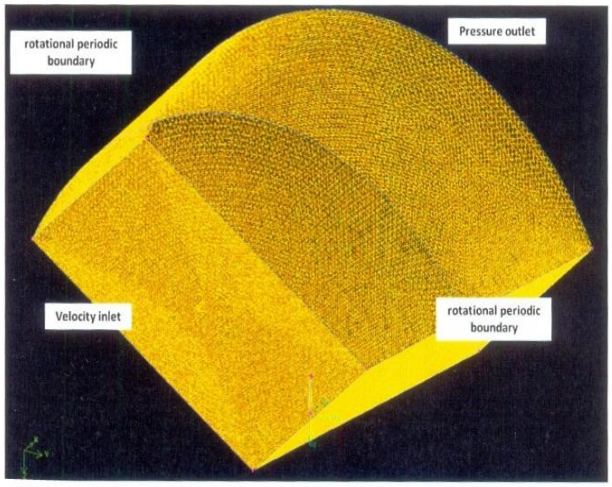

Fig.4- Grid with boundary conditions (scale 1:0.002)

3.4.3 Analysis Cases

In Figure 4shows the boundary conditions imposed: at the inlet face and at the lateral boundary undisturbed uniform wind velocity and turbulence were fixed; static pressure was set at the outlet; no -slip condition wasselected for the blade surface.

Table 3- Analysis Cases for Single Reference Frame

Case	Wind velocity (m / s)
1	5
2	9
3	10
4	12
5 (rated)	12.1

Mesh generation has presented many difficulties, owing to the different range of geometric scales represented: length of the domain (948 m), size of the rotor (47.4 m), typical chord lengths (1.3-3.25 m), and boundary layer thickness (1-2 mm). A modular procedure for generating the grid was therefore utilized, in order to take care of the local geometric scales for all those different "levels".

A representative image of the mesh generation process is shown in Figure 4. By following this logic; a selective modification of each part that constitutes the domain is straightforward. Anyway, a critical constraint was imposed by the available computing resources, since all simulations must be run on normal personal computers. The model has been scaled down by a factor of 0.002 because of the limited resources available for computations. The final Mesh has 1,223,219 elements.

3.4.4 Moving/rotating frame of reference

For the analysis with moving/rotating frame of reference case 4 shown in Table 4 is considered

Table 4 - Analysis Cases for Moving Reference Frame (MRF)

Case	Wind velocity (m / s)	Rotational speed (rpm)	Density (kg / m^3)
1	5	15.1145	1.225
2	9	15.1145	1.225
3	10	15.1145	1.225
4	**12**	**15.1145**	**1.225**
5 (rated)	12.1	15.1145	1.225

Table 5 shows the results for non-dimensional numbers for moving reference frame at inlet velocity 12m/s

Table 5 - Non Dimensional numbers for Moving Reference Frame at inlet velocity 12 m/s

Inlet velocity (m / s)	Pressure coefficient (single Blade)		Pressure coefficient (three Blades)		Reynolds Number	
	Min	Max	Min	Max	Min	Max
12	-257.2	121.2	-397.9	19.54	0.73	190

IV. RESULTS & DISCUSSION

Fig. 5 a) and b) shows the variation of maximum and minimum dynamic pressure with respect to cross section of blade respectively. In both the graphs on X-axis cross section in mm is marked and on Y-axis maximum and minimum dynamic pressure is marked from CFD results. The graph is plotted for 5, 9, 10, 12 and 12.1 m/s inlet velocity of air.

Fig. 5 a) shows variation of maximum dynamic pressure along cross section of blade. Up to cross section of 10mm maximum dynamic pressure increases, reaches its maximum value and then after 70mm it starts decreasing. In each inlet velocity Maximum dynamic pressure is obtained at 10 mm cross section and its maximum value is 240.341 Pa at 12.1m/s inlet velocity.

Fig. 5 b) shows variation of minimum dynamic pressure along cross section of blade. There is large variation of minimum dynamic pressure along the cross section of blade. It reaches its maximum value at cross section of 10 mm i.e. minimum and maximum value of dynamic pressure is observed at 10 mm. Up to 10mm there is increase in dynamic pressure after 10 mm it again starts decreasing up to 70mm and then again increases.

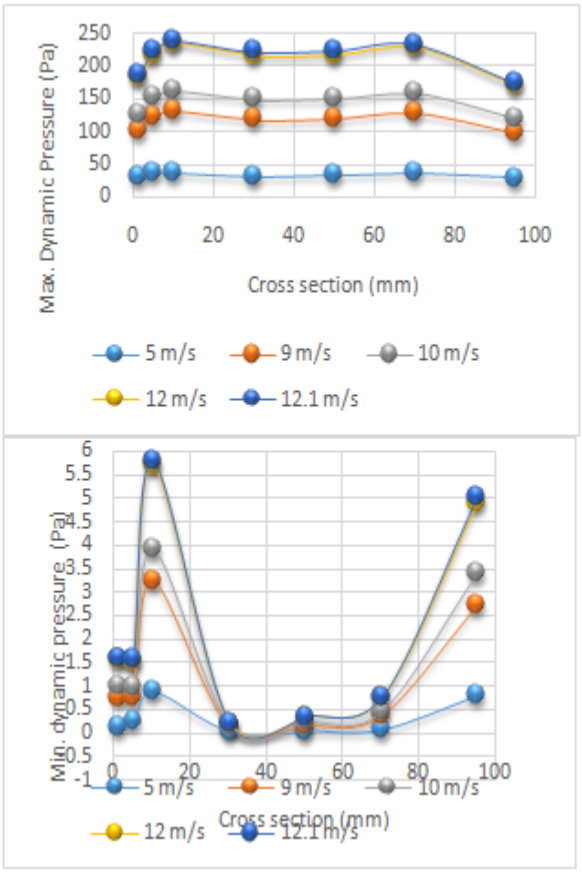

Fig.5 a) Max. Dynamic pressure Vs cross section
b) Min. Dynamic pressure Vs Cross section

Figure 6.2 a) and b) shows the variation of maximum and minimum static pressure with respect to cross section of blade respectively. Fig. 6.2 a) shows variation of maximum static pressure along cross section of blade. Up to cross section of 70mm maximum static pressure remains steady and then after 70mm it starts decreasing. In each inlet velocity, Maximum static pressure is steady up to 70 mm cross section and its maximum value is 137.079 Pa at 12.1m/s inlet velocity.

Fig. 6.2 b) shows variation of minimum static pressure along cross section of blade. Minimum static pressure is coming negative at each inlet velocity. As inlet velocity increases minimum static pressure goes on decreasing.

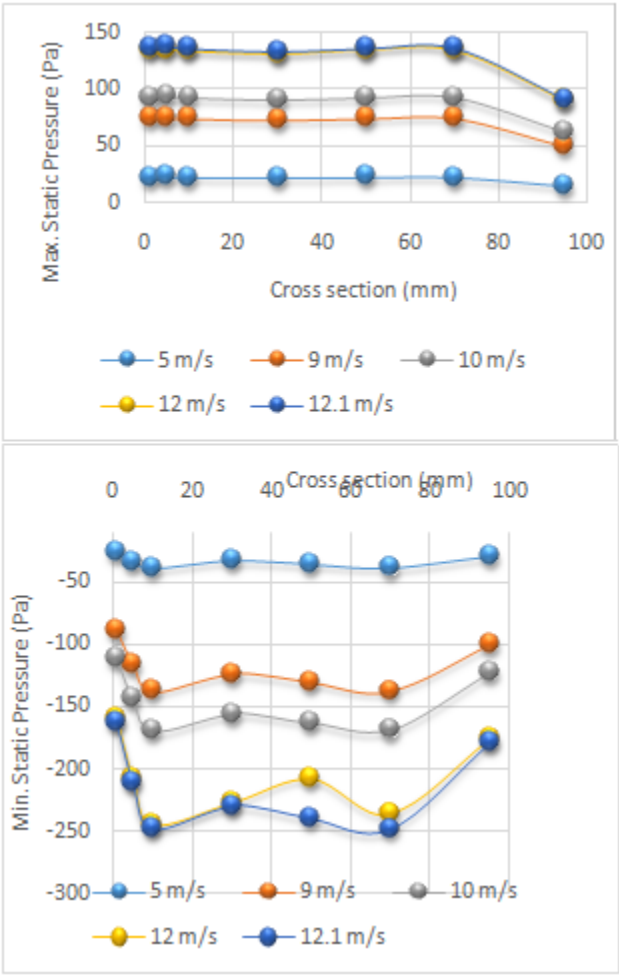

Fig.6 a) Max. Static pressure Vs cross section
b) Min. Static pressure Vs Cross section

V. CONCLUSION

This study has addressed many issues which can be summarized:

[1] Use of CFD simulations to get better understanding of wind turbine blades aerodynamics and to determine the wind turbine power coefficient.

[2] The study presents a three dimensional modeling of fluid flow around horizontal axis wind turbine using Navier Stokes solvers. Due to periodicity, only one third of the turbine rotor is modeled in the single reference frame. The simulations are performed using the k- ε turbulence model and finite-volume method. The pressure distribution on the turbine blades, near and far wakes characteristics and the power coefficients are obtained in this study.

[3] By comparing the maximum power coefficient, CFD predicted about 3.5% higher value than GF1-Bladed and Reynolds number distribution is presented for all of the wind conditions.

VI. FUTURE SCOPE

Future work should include use of higher performance computers in order to solve a full scaled model and much more elements in the computational grid, use more sophisticated meshing techniques to create hexahedral elements (surface models), tetrahedral elements (solid models) and refinement of boundary layer for achieving more accurate results, use k – ω SST turbulence model for RANS method and perform more extensive unsteady computation analysis using large eddy simulations (LES).

REFERENCES

[1] R. Lanzafame, M. Messina (2007) "Fluid dynamics wind turbine design: Critical analysis, optimization and application of BEM theory", Renewable Energy, PP- 2291-2305

[2] V. Esfahanian , A.SalavatiPour , I.Harsini , A.Haghani , R.Pasandeh , A.Shahbazi , G. Ahmadi, (2013), "Numerical analysis of flow field around NREL Phase-II wind turbine by a hybrid CFD/BEM method", Wind Engineering and Industrial Aerodynamics, PP- 29-36

[3] L. J. Vermeer, J.N. Sorensen, A. Crespo (2003), "Wind turbine wake aerodynamics", Progress in Aerospace Sciences, 2003, PP- 467-510

[4] M. O. L. Hansen, J. N. Sorensen, S. Voutsinas, N. Sorensen, H. Aa. Madsen (2006), "State of the art in wind turbine aerodynamics and aeroelasticity", Progress in Aerospace Sciences, PP- 285-330

[5] JersonRogerioPinheiroVaz, Joao Tavares Pinho, Andre Luiz AmaranteMesquita, "An extension of BEM method applied to horizontal-axis wind turbine design", Renewable Energy, PP- 1734-1740

[6] R. Lanzafame, M. Messina (2011), "BEM theory: How to take into account the radial flow inside of a 1-D numerical code", Renewable Energy, PP- 440-446

[7] R. Lanzafame, S. Mauro, M. Messina(2012), "Wind turbine CFD modeling using a correlation-based transitional model", Renewable Energy, PP- 31-39

[8] Hua Yang , Wenzhong Shen , Haoran Xu , Zedong Hong , Chao Liu, "Prediction of the wind turbine performance by using BEM with airfoil data extracted from CFD", Renewable Energy, PP- 107-115

[9] S Khelladi, N. E. BibiTriki, Z. Nakoul, M. Z. Bessenouci (2014), "Analysis and study of the aerodynamic turbulent flow around a blade of wind turbine", Physics Procedia, PP- 307-316

[10] I.S.Hwang, W.Kang, S.J.Kim (2013), "High Altitude Cycloidal Wind Turbine System Design", Procedia Engineering, PP- 78-84

[11] C. J. Bai, F. B. Hsiao, G. Y. Huang, Y. J. Chen (2013), "Design of 10 kW Horizontal-Axis Wind Turbine (HAWT) Blade and Aerodynamic Investigation Using Numerical Simulation", Procedia Engineering, PP- 279-287

[12] H. Hamdi , C. Mrad , A. Hamdi, R. Nasri (2014), "Dynamic Response Of A Horizontal Axis Wind Turbine Blade Under Aerodynamic, Gravity And Gyroscopic Effects", Applied Acoustics, PP- 154-164

[13] SarunBenjanirat, Lakshmi N. Sankar, "Evaluation Of Turbulence Models For The Prediction Of Wind Turbine Aerodynamics", PP- 1-11

[14] Yen-Pin Chen (2011), "A Study of the Aerodynamic Behavior of a NREL phase VI Wind Turbine using the CFD Methodology",

[15] Peter J. Schubel, Richard J. Crossley (2012), "Wind Turbine Blade Design", Energies, PP- 3425-3449

[16] Stefan S. A. Ivanell (2009), "Numerical Computations of Wind Turbine Wakes", Stockholm,

[17] Bumsuk Kim, Woojune Kim, SungyoulBae, Jaehung Park and Manneung Kim (2011), "Aerodynamic design and performance analysis of multi-MW class wind turbine blade", Journal of mechanical science and technology,

[18] Fluent 12.0 Documentation, Users guide, Technical Report, ANSYS Inc.